

Article

Energy Benefits of Tourist Accommodation Using Geodesic Domes

Ángel Benigno González-Avilés *, Carlos Pérez-Carramiñana, Antonio Galiano-Garrigós and María Isabel Pérez-Millán

Building Construction Department, Polytechnic School Alicante, University of Alicante, 03690 Alicante, Spain; c.perez@ua.es (C.P.-C.); antonio.galiano@ua.es (A.G.-G.); isabel.perez@ua.es (M.I.P.-M.)

* Correspondence: angelb@ua.es; Tel.: +34-65-315-48-91

Abstract: Over the last decade there has been a proliferation of glamping architecture. This study analyses the energy performance of geodesic domes for use in tourist glamping compared to more conventional prismatic architectural solutions. The energy analysis of geodesic domes applied to this type of singular construction project currently lacks detailed studies that provide conclusions about their relevance and suitability with respect to other types of architecture. The main objective of this research is to demonstrate the energy benefits of tourist accommodations that use geodesic structures compared to those with a simple geometry. A comparative study of a traditional and a geodesic geometry accommodation is carried out, considering that they share the same characteristics and they are built with the same construction solution. An energy simulation of both architectures is carried out by using DesignBuilder software. The most influential strategies, such as Direct Passive Solar Gain, Heating, Natural Ventilation Cooling, Fan-Forced Ventilation Cooling and Window Solar Shading are considered. After demonstrating the greater efficiency of geodesic domes, this study analyses the relevance of subdividing the accommodations into several geodesic dome spaces. The results quantify an energy benefit of 52% for cooling consumption using the geodesic dome solution compared to a traditional prismatic solution.

Citation: González-Avilés, Á.B.; Pérez-Carramiñana, C.; Galiano-Garrigós, A.; Pérez-Millán, M.I. Energy Benefits of Tourist Accommodation Using Geodesic Domes. *Buildings* **2024**, *14*, 505. <https://doi.org/10.3390/buildings14020505>

Academic Editors: Cristina Carpino, Miguel Chen Austin, Dafni Mora and Natale Arcuri

Received: 6 December 2023

Revised: 17 January 2024

Accepted: 18 January 2024

Published: 12 February 2024



Copyright: © 2024 by the authors. Licensee MDPI, Basel, Switzerland. This article is an open access article distributed under the terms and conditions of the Creative Commons Attribution (CC BY) license (<https://creativecommons.org/licenses/by/4.0/>).

Keywords: energy efficiency; thermal comfort; glamping; geodesic domes; simulation

1. Introduction

Glamping, or glamorous camping [1], is a current word that started as a new form of accommodation in Africa [2]. It is defined as the global phenomenon that combines the experience of camping in the open air with the luxury and conditions of the best hotels.

It is also worth noting that the relationship between the concepts of pandemic and travel has been amply demonstrated throughout history [3]. The latest research shows that since COVID-19, the purchase of glamping-type travel plans has reached 45.9%, compared to 24.7% [4] for hotel/resort stays. The European trend for the use of this new camping style is booming [5], and has a monetary return in Europe of USD 965.7 M (Figure 1). For the period 2023–2030, a compound annual growth rate (CAGR) of 10.9% [6] is expected.

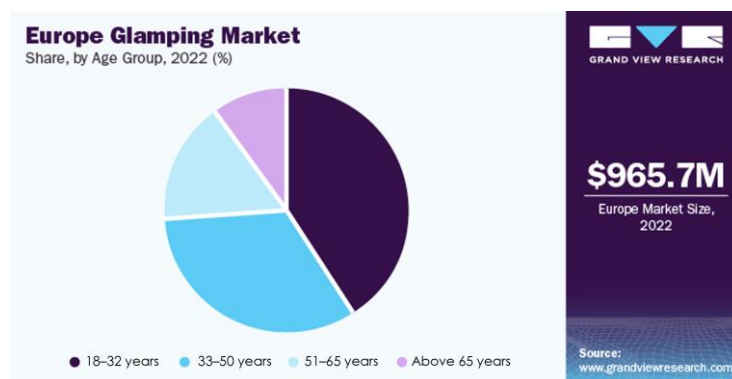


Figure 1. European glamping market in 2022 [6]. Source: Europe Glamping Market Size, Share and Growth, 2023.

The research by Claver-Cortes et al. [7] has significantly related these performance levels to environmental proactivity and their implications for policy makers. An increasing number of hotels are engaging in greater environmental stewardship [8]. This leads to economic benefits, in terms of resource savings and an image of commitment to the environment. Another reason is the new public pressure exerted by many environmentally conscious consumers [9]. In general, middle-aged tourists are more environmentally conscious and are willing to pay more for accommodations that consider renewable energy sources [10]. Travelers interested in this type of tourism want quality services, different experiences and open spaces in quiet places [11]. As opposed to mass tourism, they are looking for an individual or small-group approach in sustainable areas that protects and respects nature [12]. This evolution of the tourism market requires new permanent accommodation structures, which usually have a significant environmental impact [13]. These accommodations tend to have a higher price tag; however, considering their increasing occupancy rates, it is noted that their high price does not diminish their attractiveness [14].

This research focuses on two types of permanent housing based on a clear geometrical distinction (Table 1). On the one hand, prismatic architecture, more closely related to industrialised huts with straight geometries, is studied. On the other hand is the geodesic dome, on which this study focuses.

Table 1. Examples of recent prismatic architecture and geodesic domes. Source: Archdaily.

Tenir Eco Hotel [15] Levelstudio	DOM(E) [16] NRJA Architects
Labt 20 Modular home [17] Borrachia + GB Architects	Geodesic house [18] Ecoprojecta
M+J House [19] Manuel Cerdá Architect	Sazae Sauna [20] Kengo Kuma & Associates
Ranwu Lake campsite [21] Xiao Yin Architecture Design Firm	Two domes and a plinth: House 8 [22] B+V Architects
Cambará Container Housing [23] Saymon Dall Alba + Mégui Dal Bó	In progress: Domo Cluster [24] Arketiposchile

The current literature has presented scattered data regarding the reduced use of materials, particularly from a structural point of view [25,26]. However, these studies

have mostly focused on large-span spaces, like planetariums [27] or public areas [28]. Some energy studies may have exhibited a bias towards roof solutions [29] or the advantages or benefits of the application of a dome structure for tourist education facilities [30]. The novelty of this research lies in its quantification of the energy savings of this type of architecture when applied to domestic or tourist accommodation spaces.

1.1. The Relationship between Efficiency and Geometry as a Research Objective

The main objective of this research is to demonstrate the energy benefits of housing with geodesic structures compared to a parallelepiped geometry. This demonstration is carried out by comparing three housing units: one with a traditional parallelepiped geometry and two housing units with geodesic geometry, all executed with the same construction solution, the same surface area and in the same climate. An energy simulation of the three designs is carried out for the volume of the parallelepiped geometry, the single geodesic dome and the double geodesic dome. The software used is DesignBuilder [31] (version v.7.0.1.006, DesignBuilder Software Limited, Stroud, UK). This software allows for the simulation of energy efficiency and thermal comfort in buildings using the EnergyPlus v.23.1.0 calculation engine [32]. This software also provides computational fluid dynamics (CFD) calculations with which to simulate the average radiant temperature distribution, the operating temperature and the estimated thermal comfort in different zones within the building. For the computer simulations, the thermal transmittances of the façade and the air infiltration through the window frames, measured in situ, are considered. The air infiltration is low, due to the small proportion of the openings in the façade and the characteristics of the wooden frames used.

It will be concluded whether this type of construction solution really provides an energy/economic benefit compared to a more traditional geometrical solution.

1.2. History of the Geodesic Dome

We can define a geodesic dome as part of a geodesic sphere. A polyhedron generated from an icosahedron or a dodecahedron can also be generated from any of the Platonic solids [33]. The faces of the regular Platonic solids are regular polygons equal to each other. Based on this description and Euler's theorem, the cube, tetrahedron, octahedron, dodecahedron and icosahedron are Platonic solids, being the only five bodies that fulfil the properties described by the theorem and that maintain the constant [34].

The Jena planetarium designed by Walther Bauersfeld in 1922 is considered to be the first geodesic dome in the world [35]. However, it is Richard Buckminster Fuller who is considered the father of geodesic structures [36]. In 1949, Fuller erected a dome capable of supporting its own weight without limit [37], and patented it in 1951 [38]. This structure was supported by the principles of tensegrity structures. It comprised a diameter of 4.2 m, was constructed of aluminium tubes (Figure 2) and covered with a vinyl coating. Years later, the US Army took advantage of the qualities of these structures. After several commissions for the army, Fuller built his own house in Carbondale (IL, USA). However, at the time, Fuller's aim was not a concern for the environment but a strategy to reduce the cost of housing [39]. Fuller also designed the US pavilion for the World Expo in Montreal in 1967, with a structure 76 m in diameter and 62 m high. The dome consisted of an interior division of seven levels, with the structure and envelope made of steel and polymers [40].



Figure 2. Demonstration of the strength of the dome; Buckminster Fuller and students hang from sections of the dome [41].

In June 1979, the American Institute of Architects (AIA) awarded Fuller the gold medal [42], considering the geodesic dome to be “the strongest, lightest and most efficient means to enclosing space yet known”. Leonhard Euler, in 1750, expressed in his polyhedra theorem the existence of only five regular polyhedra, which maintain the constant $c = 2$ that relates the faces, vertices and edges of these polyhedra [43]. The regularity of the elements that make up the Platonic solids allows for the generation of geodesic domes by allowing for the division of their faces while maintaining the relationship of the elements that make them up. Depending on how it is generated, there are three types of geodesic domes: Class I, Class II and Class III [44]. Most geodesic domes constructed are either Class I or II, due to the availability of the methods that generate tessellations with a linear increase in complexity. Class I are the easiest to use, especially when near equatorial truncation is desired. In Figure 3 we can see the different models of Class I geodesic domes, depending on their frequency from one to six.

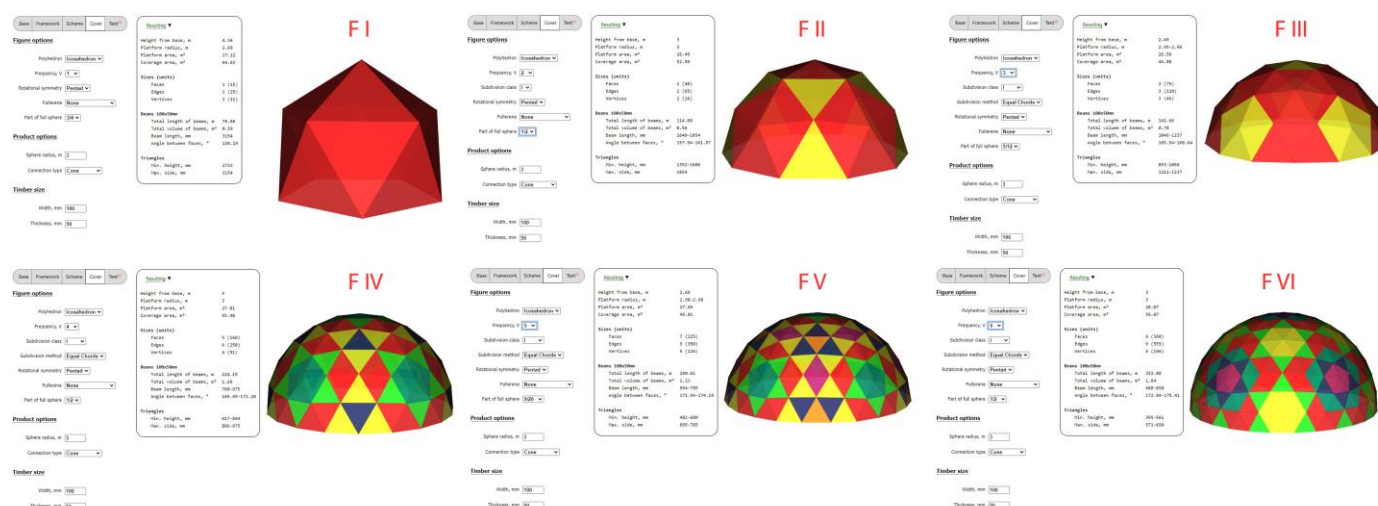


Figure 3. Models of Class I geodesic domes depending on their frequency from I to VI. Source: own elaboration from www.acidome.ru (accessed on 3 December 2023).

1.3. Geodesic Domes' Geometrical and Energetic Characteristics

The dome is the geometric shape that encloses the greatest amount of volume with the least amount of surface area. This results in important savings (greater than any other structure with a different shape) in the building materials used to enclose a usable work area.

A dome, as a spherical shape, has less surface area per unit of internal volume; thus, it reduces temperature gains or losses through its enclosure. The forces applied to the dome are distributed throughout the structure, generating a stable and solid construction [45], although it is true that hemispherical domes considerably increase the final weight compared to a 1/3 or 2/3 [46] span. It has a uniform weight distribution on the ground plane and a low centre of gravity, resulting in a structure with great seismic resistance. Its materiality is mainly based on lightweight materials, such as wood or steel, which are connected to each other by means of prefabricated or dry construction processes. This type of structure is no longer considered a high-tech construction system, as it is based on low-tech construction protocols and schemes [47], allowing for faster construction compared to that of other conventional structures.

In short, geodesic domes offer a wide range of possible uses due to the qualities described above. Geodesic domes have proven to be such a flexible architectural form, they have housed everything from radar equipment to radical back-to-landers [35]. They can solve both ephemeral needs, such as the construction of domes for one-off events, auditoriums, etc., or permanent needs for residential use; they can also be used in agriculture, as they concentrate light more efficiently than a conventional greenhouse dome [46,48]. The speed of the execution of their structure allows for the transport and construction of resistant shelters, even those with military applications. Moreover, no in-depth studies of spherical trigonometry or stereographic projections [49] are required for their design or construction. This is why, in recent years, their use as accommodation has proliferated so much. An example of their efficiency is the study of the Hotel Ecocamp in Patagonia (Chile), a pioneer project in the construction of hotel rooms with geodesic domes. Soares [42] has estimated that savings of 30% on materials and 50% on heating energy could be achieved compared to other conventional examples in the same area. Other examples in Europe are the Aurora Dome (Finland), Whitepod (Switzerland) or the geodesic domes designed by the Ecoprojecta [50] studio in the towns of Yecla and Jumilla (Murcia) in Spain.

Our research aims to demonstrate and quantify the energy savings with this type of structure compared to conventional models. This study supports the energy and economic benefits of geodesic projects designed to have a lower environmental impact on rural areas, and offers more solutions about how to improve the energy efficiency of domes and solar performance [51,52].

2. Materials and Method

Geometrical studies offer us very important variables on which to base this study. The most significant are the floor area, the envelope area and the length of the edges. The research by Hagh Nazar et al. [53] has already highlighted differences in edge length and other aspects which are differentiated according to frequency. Determining the optimum geometry design for geodesic domes presents difficulties, due to the fact that the height of the dome keeps on changing during the design process [54]. In order to understand the differences, depending on the frequency used, a geodesic dome with a radius of 3 m has been studied and is shown in Figure 3. Frequency I allows for a greater height from the base (4.34 m) but, on the other hand, a smaller floor area (17.12 m²). For frequencies II, IV and VI, the height coincides with the radius of the inscribed circumference (3 m), and the surfaces are very close to 27 m². Frequency III has the lowest free height and would not be occupiable (2.49 m), which is very similar to frequency V (2.69 m).

Fuller's first argument for the energy efficiency of domes was the smaller surface area per unit volume guaranteed by their spherical geometry [55]. This results in a smaller surface area exposed to cold in winter and heat in summer compared to other architectures in the same space. Additionally, the continuous air flow inside the dome, with no stagnant corners, requires less energy to circulate the air and maintain uniform temperatures [56].

The dome combines the inherent stability of triangles with the advantageous volume/surface area ratio of a sphere, which results in less building materials to include more space. There is an estimated 30% reduction in materials and 50% reduction in energy compared to a conventional masonry construction [57] on the same built area, or 25–30% compared to metal [58].

2.1. Case Studies

Three different case studies located in the same climate zone BSh (cold semi-arid) of the Köppen climate classification have been analysed for this research:

- Case study 1: reference block. It is a simplified model of a traditional construction with dimensions of 10 m wide, 7.72 m deep and 3.5 m high, with an occupation surface of 77.2 m², 201.3 m² of envelope and 77.2 m² in contact with the ground. It consists of a single living area, an access door and glazing corresponding to 10% of the surface area of each façade. This parallelepiped shape has been very common in modern architecture in recent years. Many examples can be found on the leading architecture portals, such as Archdaily [59]. Some projects of this type of prismatic volumetry are the Tenir Eco hotel, the Labt 20 modular housing, the M + J house, the prototypes of the Lago Ranwu campsite or the Cambará Container House, among others (Table 1). The energy efficiency of this type of architecture has been widely studied [60], as well as its spatial uses [61], its structural capacity [62] and its reuse [63].

These architectures seek to minimise the resources employed to create residential units that meet energy and comfort standards, but also offer a cost-effective option in the architectural market.

- Case study 2: geodesic dome with a 5m radius and frequency IV, with a surface occupation of 77.2 m² equal to the reference block (case study 1), 154.11 m² of envelope and 77.2 m² in contact with the ground.
- Case study 3: two smaller geodesic domes (3 m radius with 27.8 m² of surface area and another with a 4m radius and 49.4 m² of surface area) with a total surface area of 77.2 m² (27.8 + 49.4) equal to the reference block (case study 1). In this case study, a differentiation of uses is considered; to this end, one dome is designed for night use (bedroom) and the other for day use (living room). This distinction means that both the electronic devices capable of generating heat for occupancy during the day and night hours will be different, making it possible to quantify the differentiable impact on energy consumption with respect to other case studies (with a single envelope).

For the comparison between the different case studies (Figure 4), it was decided to disregard the existence of interior partitions, in order to check for the volumetric implication of the energy analysis. The same orientation was used in all three case studies. Every façade was designed with the same proportion of openings in each orientation.

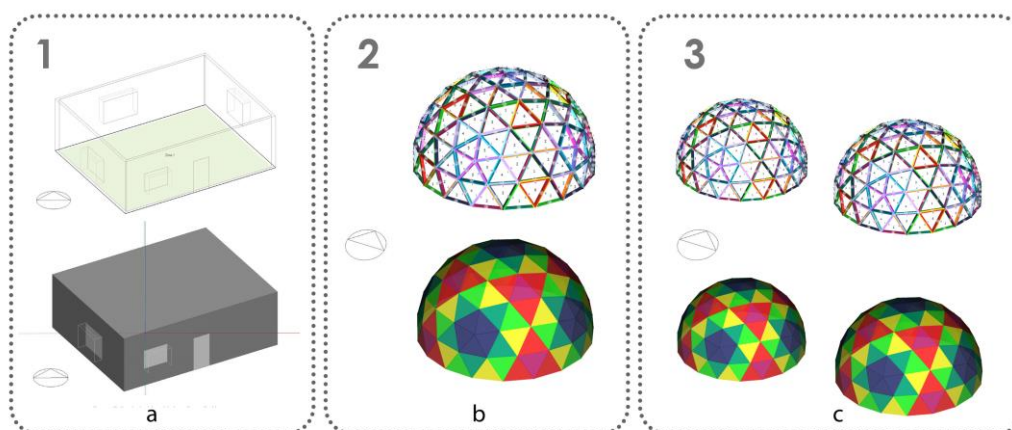


Figure 4. Case studies. (a) Case 1: reference block, (b) case 2: geodesic dome and (c) case 3: double geodesic dome. Source: own elaboration using DesignBuilder software.

2.2. Morphological Analysis of the Geodesic Dome

Several recent studies have calculated the optimal geometry for this type of single-layer architecture and its algorithm [54], or have studied its optimisation in the face of earthquakes [64]. In the field of structures, this type of architecture has been extensively studied [65–68]. However, in the residential field, due to their thermal characteristics, domes have a great potential that has yet to be studied.

In chronological order, the first dwellings to use this type of geometry were the Easy Domes by architect Kári Thomsen and engineer Ole Vanggaard in 1992. This was followed by the Genesis Project as a temporary home for homeless people in Los Angeles in 1993, Aso Farms in Japan in 1995, Domo House in Oregon, the hemispherical houses of Solaleya and The Inn Place in Brenham in Texas in 2006 [69] and, more recently, the superposition of several domes, such as the Domo Cluster by Arketiposchile [24] in 2012 and the geodesic dwelling by Ecoproyecta [50] in 2016.

This work aims to identify whether the use of domes produces energy savings and the thermal qualities inherent to their morphology. For this purpose, different analyses are carried out by modifying different calculation parameters for the materials used and the construction solutions employed. The demand for air conditioning, cooling and comfort conditions is included in two models (case studies 2 and 3). This will be compared to the geometry of a parallelepiped house with the same surface area (case study 1).

This study is based on a frequency IV 1/2 dome for a single-family house with the same surface area as for cases 1 and 2. The progress of this research will make it possible to determine the convenience of dividing the surface area into smaller domes, thus, sectioning the uses of the house, as in case 3. In addition, a detailed study is also carried out on the behaviour of the materials used, the construction solutions employed and how these decisions affect the thermal behaviour of the architectural complex.

All this is carried out using the energy analysis software DesignBuilder v.7.0.1.006, assessing which is the best solution and whether it really represents a sustainable improvement compared to traditional construction.

To do this, it is considered essential to determine the most appropriate length for the crosspieces that make up the structure of the dome, as this will condition the existing joint metres for this morphological solution and, therefore, the infiltrations. It is important to add, at this point, that this aspect can be reduced depending on the type of frequency used. Frequency IV 1/2 uses a greater number of edges (712) than frequencies III 5/12 (225) or III 7/12 (315). Frequency IV 1/2 is chosen as the most unfavourable case. It is also considered essential to consider the spatial suitability of the total volume generated. At frequency IV 1/2 the clear height is 5 m.

At the construction level, the geodesic dome is made up of triangular pieces pre-assembled in a workshop. These pieces are placed edge by edge on site. The construction process is carried out in situ and dry-jointed (Figure 5).

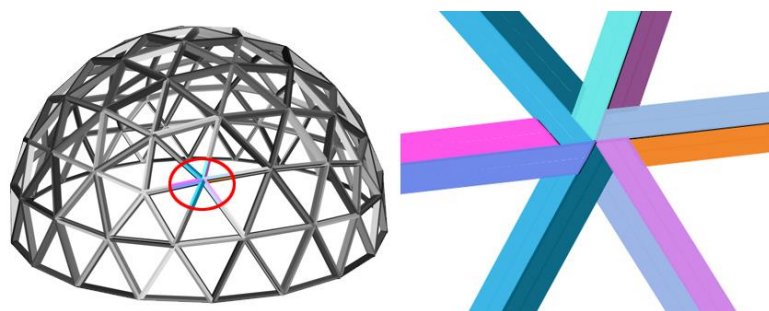


Figure 5. Wooden joints used in case studies 2 and 3.

The virtual representation of the dome under study is a fundamental element for understanding its application and behaviour. However, in addition to its morphological information, it is essential to add specific structural information in order to obtain a more exhaustive and operative control both of the manufacture and of the subsequent construction of the geodesic dome. This information is obtained by introducing different variables into the Geodesic Dome Calculator web platform [70], obtaining a structural BIM model with the complete dimensioning of each of the crosspieces, their layout, cutting angles and vertex junctions, as well as the representation of the flat faces of the dome (Figure 6a). It is also necessary to draw in detail the heights of each of the bars with respect to the 0 level (base plane) on which they must be placed (Figure 6b).

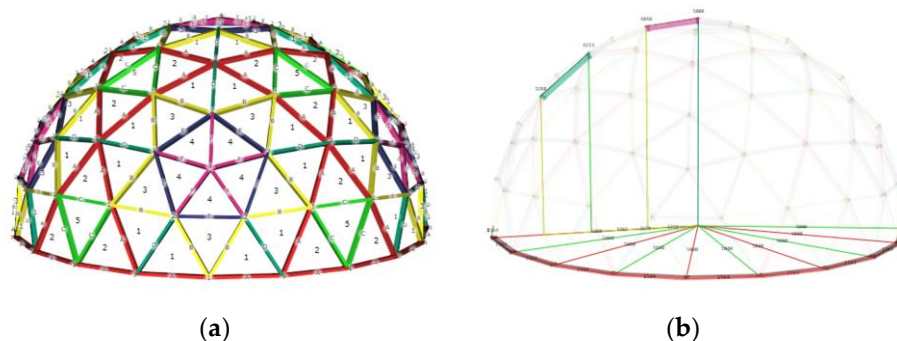


Figure 6. Virtual representation of the dome: (a) designation of bars, faces and vertices; (b) 3D bar placement scheme. Source: own elaboration from www.acidome.ru (accessed on 3 December 2023).

As mentioned above, the hemisphere used is of frequency IV, so that the base is completely parallel to the horizontal plane. An icosahedron is, therefore, used as the base platonic solid. Each of the above representations provides specific information for the machining and prefabrication of the construction elements, and can be used to automate the processes or to carry them out in a more efficient and controlled manner.

In addition, the data related to the real construction are also integrated into the model, considering a basic façade module (Figure 7a) formed by the following:

- A triangular piece generated by wooden crosspieces.
- Interior thermal insulation (cellulose).
- Interior wood panel (Oriented Strand Board-OSB).
- Exterior wood panel (Oriented Strand Board-OSB).
- Interior finish (according to project requirements).
- Exterior finish (mineral-based paint).
- Joint coating (structural silicone).

The enclosure modules can also be replaced by carpentry modules to generate the façade openings (Figure 7b). Considering this, it is possible to interact with the enclosure by modifying its conditions, materiality and components, by means of the geodesic dome modulation.

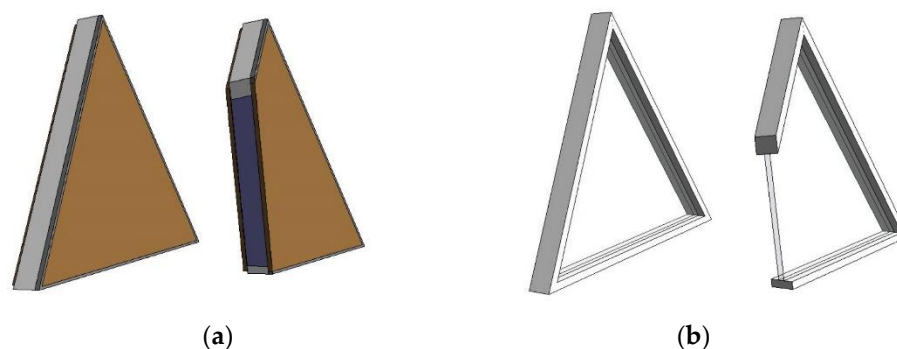


Figure 7. (a) Representation of facade constructive module; (b) representation of carpentry constructive module. Source: own elaboration using Autodesk Revit software v.2020.1.

As a result, a virtual model is obtained with which to document and visualise the construction of the dome, to quantify and prefabricate the resulting modules, and also to provide morphological and spatial relationships for further comparison to traditional geometries.

When considering a similar geometrical solution, it is essential to bear in mind that the usable space in the interior of a dome will be smaller. This is due to the fact that the lower ring, 97 cm high and 35 cm deep, is a non-habitable volume to be subtracted from the total (Figure 8). Fuller, in his Carbondale dwelling, used this depth as a bookcase.

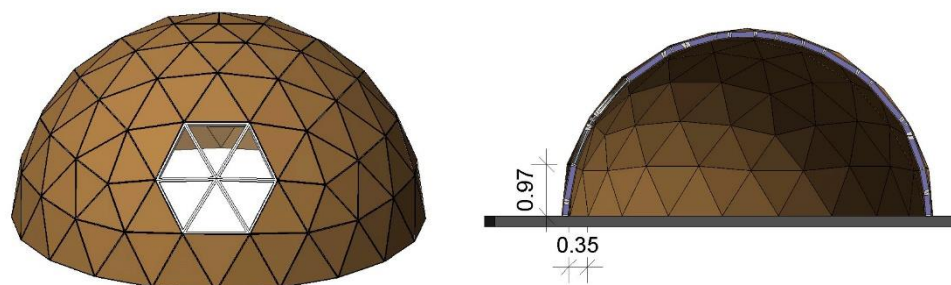


Figure 8. Global view and section of the virtual model. Source: own elaboration using Autodesk Revit software v.2020.1.

2.3. Energy Analysis of the Geodesic Dome

In recent years, computational geometry has allowed for a new formulation of the geometric bases and numerical procedures used to generate any type of spatial dome [71]. Today, digital tools are crucial for the design and manufacture of this type of non-rectilinear geometry [72]. This is why, in addition to the energy analysis of the geodesic dome, this research considers how construction costs have a direct influence on whether a house is considered to be sustainable or not.

Therefore, the Autodesk software REVIT 2020.1 and the visual programming application Revit Dynamo v.2.6.1 are used as the parametric modelling tools for the development of this research (Figure 9).

```

//This is a very important step. It is the triangulation function that will divide
def tri(sur:var)
{
  c1=sur.PerimeterCurves();
  p1=c1.PointAtParameter(0);
  p2=c1.PointAtParameter(0.5);
  c1=Surface.ByPerimeterPoints([p1[0],p2[0],p2[2]]);
  s2=Surface.ByPerimeterPoints([p1[1],p2[1],p2[0]]);
  s3=Surface.ByPerimeterPoints([p1[2],p2[2],p2[1]]);
  s4=Surface.ByPerimeterPoints([p1[0],p2[1],p2[1]]);
  returns={s1,s2,s3,s4};
};

R:=#(0.600);
Rad=(r*(Math.Sin(72)))/(2*Math.Sin(36));
theta=List.DropEveryNthItem(0.296.26,2,0.1);
p1=Point.BySphericalCoordinates(CoordinateSystem.Identity(),90-Math.Atan(0.5),theta);
p2=Point.BySphericalCoordinates(CoordinateSystem.Identity(),90-Math.Atan(-0.5),theta);
g1=List.Flatten(List.AddItemToEnd(Point.ByCoordinates(0,0,r)*c1),(List.DropItems(L
p2=List.Flatten(List.AddItemToEnd(Point.ByCoordinates(0,0,r)*c1),(List.DropItems(L
g2=Flatten(Transpose((List.DropItems(List.Sublists(p1,0.1,1),1),List.DropItems(L
g4=Flatten(Transpose((List.DropItems(List.Sublists(p2,0.1,1),1),List.DropItems(L
s1=Surface.ByPerimeterPoints(List.Flatten([g1,g2,g3,g4],1));

//Now we will now make a sphere that also uses the variable R. The idea is to inscrib
sp=PolySurface.BySolid(Sphere.ByCenterPointRadius(Point.Origin(),R));

//Once we have our triangulation function set up, we can triangulate the inscribed
s2=tri(Flatten(tri(s1)));
c1=s2.PerimeterCurves();

//Then we can get the points at each vertex:
p3=c1.PointAtParameter(0);

//Now we can project the points on the surface of the sphere:
p4=Flatten(p3.Project(sp,Vector.ByTwoPoints(Point.Origin(),p3))*1x2);

//To create a geosphere, all we need to do is to make triangle surfaces out of th
s3=Surface.ByPerimeterPoints(p4);

//The final step is to turn the geosphere into a geodesic dome:
h1=Flatten(List.FilterByBoolMask(s3,s3.PointAtParameter(0.5,0.5).Z<0)*c1);
h2=PolySurface.ByJoinedSurfaces(h1);

```

Figure 9. Code for frequency IV geodesic dome generation. Source: own elaboration using Dynamo.

Autodesk REVIT, like its counterparts from other commercial companies, allows for the creation, visualisation and documentation of parametric virtual models which are very close to the construction reality. By means of the Autodesk REVIT software, the envelope studied is modelled “AsBuild”, obtaining material calculation tables that are faithful to the construction reality and allow for the costs and construction times to be determined with greater precision.

Different simulation options were considered for carrying out the proposed energy analysis (Open Studio, Therm, ECOTECT, Lider-Calener HULC, etc.); after rejecting those tools that had certain limitations when analysing complex geometries and/or compatibility issues with other modelling software, the Climate Consultant v.6.0 and DesignBuilder v.7.0.1.006 applications were finally chosen.

Climate Consultant provides detailed climate information for specific locations by reading EPW [32] (Energy Plus Weather) formats. It allows for an understanding of how lighting, ventilation and thermal comfort affect the design. DesignBuilder is a software that integrates the EnergyPlus [33] calculation module, and is one of the most advanced tools in this field of architectural design.

EnergyPlus was developed in the United States and is continuously updated; it contains climate data files even up to hourly and sub-hourly levels [73]. This energy calculation and simulation engine requires graphic interfaces, such as DesignBuilder, OpenStudio, Ecotect, etc., for its understanding and use, due to the complexity of the data.

With regard to the air conditioning/cooling demand, the energy requirements necessary to satisfy the comfort conditions (both for air conditioning or cooling) will be obtained. Energy Plus allows for the detailed incorporation of HVAC (heating, ventilation and air conditioning) installations to assess energy performance, thermal comfort and energy efficiency. The programme considers the summer and winter periods to establish calculation priorities. All indoor environmental conditions within the living area were studied, according to the climate data collected from Climate Consultant.

In relation to the comfort conditions, the calculation of the comfort/discomfort hours inside the living spaces will be carried out by means of the standardised calculation parameters of the ASHRAE (American Society of Heating, Refrigerating and Air-Conditioning Engineers) Standard 55 [74]. For the thermal balance, the thermal gains are shown considering different factors: solar, occupancy, thermal transmittance of the

envelope, etc. The value of the renovations/hour required for each space is also obtained, as well as the necessary infiltration flow rate due to natural ventilation.

In short, for this study, first of all, a geometric model is created in DesignBuilder and the data obtained are analysed according to certain established parameters (thermal bridges, materiality, thermal resistance, meeting solution and carpentry solution); subsequently, a series of comparative analyses are carried out, modifying the different parameters mentioned above to adapt them to the construction and economic needs that may exist for a project with these characteristics. It also studies the different constructive casuistry that can damage the energy performance of this type of housing, making a comparison to a traditional house with similar characteristics.

3. Results

3.1. Climatic Study of the Area

The geographical location of the project is fundamental for the analysis of the EPW metadata associated with the site, as well as the actual orientation and the orientation of the project. The location of the case studies is the high plateau area of Murcia (Spain), as it is the actual location of two geodesic dome projects executed by the architectural firm Ecoproyecta. The area in which they are located corresponds to the climate zone Bsh (cold semi-arid) of the Köppen climate classification. For the climatic analysis, the data used are those collected by the nearest climatic station in the region of Murcia, very close to the work area (Figure 10).

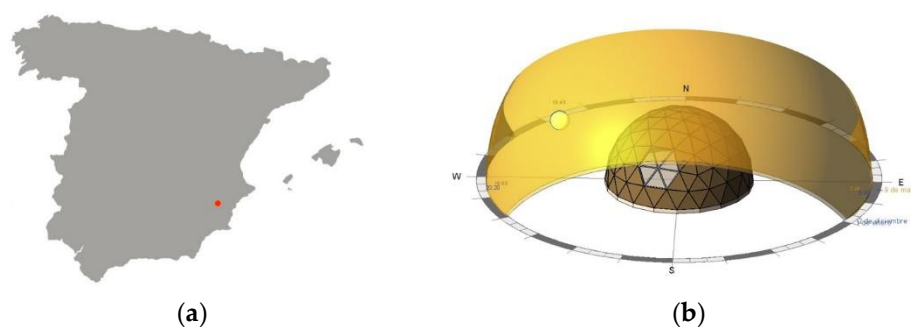


Figure 10. Location (a) and orientation (b) of case studies. Source: own elaboration using Autodesk Revit software.

The calculation assumes that the user adjusts to the climate by wearing the appropriate clothing, such as a sweatshirt and long trousers in winter and lighter clothing in the summer months. Additionally, a metabolic activity level of 1.1 met is assumed, which corresponds to sedentary activities. The rest of the values are obtained from “ASHRAE Standard 55, current Handbook of Fundamentals Comfort Model” (Figure 11).

ASHRAE Standard 55, current Handbook of Fundamentals Comfort Model (select Help for definitions)	
1. COMFORT: (using ASHRAE Standard 55)	
1.0	Winter Clothing Indoors (1.0 Clo=long pants,sweater)
0.5	Summer Clothing Indoors (.5 Clo=shorts,light top)
1.1	Activity Level Daytime (1.1 Met=sitting,reading)
90.0	Predicted Percent of People Satisfied (100 - PPD)
20.3	Comfort Lowest Winter Temp calculated by PMV model(ET* C)
24.3	Comfort Highest Winter Temp calculated by PMV model(ET* C)
26.7	Comfort Highest Summer Temp calculated by PMV model(ET* C)
84.6	Maximum Humidity calculated by PMV model (%)
2. SUN SHADING ZONE: (Defaults to Comfort Low)	
23.8	Min. Dry Bulb Temperature when Need for Shading Begins (°C)
315.5	Min. Global Horiz. Radiation when Need for Shading Begins (Wh/sq.m)
3. HIGH THERMAL MASS ZONE:	
8.3	Max. Outdoor Temperature Difference above Comfort High (°C)
1.7	Min. Nighttime Temperature Difference below Comfort High (°C)
4. HIGH THERMAL MASS WITH NIGHT FLUSHING ZONE:	
16.7	Max. Outdoor Temperature Difference above Comfort High (°C)
1.7	Min. Nighttime Temperature Difference below Comfort High (°C)
5. DIRECT EVAPORATIVE COOLING ZONE: (Defined by Comfort Zone)	
20.0	Max. Wet Bulb set by Max. Comfort Zone Wet Bulb (°C)
6.6	Min. Wet Bulb set by Min. Comfort Zone Wet Bulb (°C)
6. TWO-STAGE EVAPORATIVE COOLING ZONE:	
50.0	% Efficiency of Indirect Stage
7. NATURAL VENTILATION COOLING ZONE:	
2.0	Terrain Category to modify Wind Speed (2=suburban)
0.2	Min. Indoor Velocity to Effect Indoor Comfort (m/s)
1.5	Max. Comfortable Velocity (per ASHRAE Std. 55) (m/s)
8. FAN-FORCED VENTILATION COOLING ZONE:	
0.8	Max. Mechanical Ventilation Velocity (m/s)
3.0	Max. Perceived Temperature Reduction (°C) (Min Vel, Max RH, Max WB match Natural Ventilation)
9. INTERNAL HEAT GAIN ZONE (lights, people, equipment):	
12.8	Balance Point Temperature below which Heating is Needed (°C)
10. PASSIVE SOLAR DIRECT GAIN LOW MASS ZONE:	
157.7	Min. South Window Radiation for 5.56°C Temperature Rise (Wh/sq.m)
3.0	Thermal Time Lag for Low Mass Buildings (hours)
11. PASSIVE SOLAR DIRECT GAIN HIGH MASS ZONE:	
157.7	Min. South Window Radiation for 5.56°C Temperature Rise (Wh/sq.m)
12.0	Thermal Time Lag for High Mass Buildings (hours)
12. WIND PROTECTION OF OUTDOOR SPACES:	
8.5	Velocity above which Wind Protection is Desirable (m/s)
11.1	Dry Bulb Temperature Above or Below Comfort Zone (°C)
13. HUMIDIFICATION ZONE: (defined by and below Comfort Zone)	
14. DEHUMIDIFICATION ZONE: (defined by and above Comfort Zone)	

Figure 11. Editable parameters associated with the ASHRAE Standard 55 comfort model (own elaboration using Climate Consultant 6.0 software).

The range of dry bulb temperatures recorded per month in the region and the annual average range are obtained. The upper part of the grey band represents the winter comfort temperature and the lower part represents the summer comfort temperature. The green-coloured area represents the maximum and minimum temperatures. Yellow represents the average of the recorded high and low temperatures. The global average temperature can be read in the open band between the yellow shaded areas.

The software makes it possible to designate, in a simple way and for any type of project, the percentage of annual hours above or below the values recorded as comfortable. It can be seen that the average temperature in the region is around 18 °C, and that the annual temperature varies between 3 °C and 35 °C (Figure 12). It is important to add that the latest research by Espín et al. [75] warns of increasingly warmer thermal conditions in southeastern Spain, with less cold and less comfortable thresholds in winter and an increase in thermal discomfort in summer.

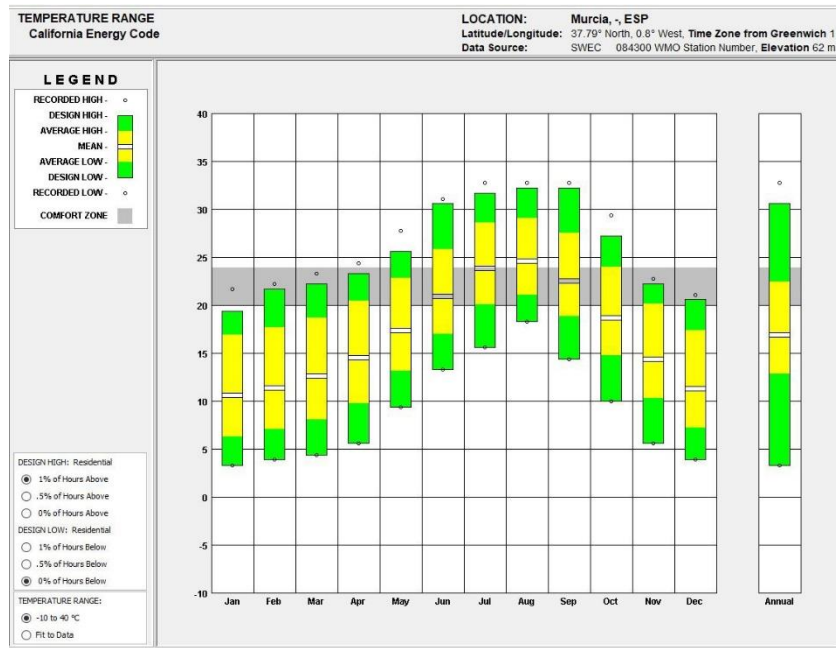


Figure 12. Simulation results: temperature range. Source: own elaboration using Climate Consultant 6.0 software.

Figure 13 represents, in two phases, the diurnal dry and wet bulb thermal variation flux per month (blue area and red lines), and the solar radiation per square metre of surface area. The maximum dry bulb temperature reaches values of 33.7v°C in August and a minimum of 2 °C in January.

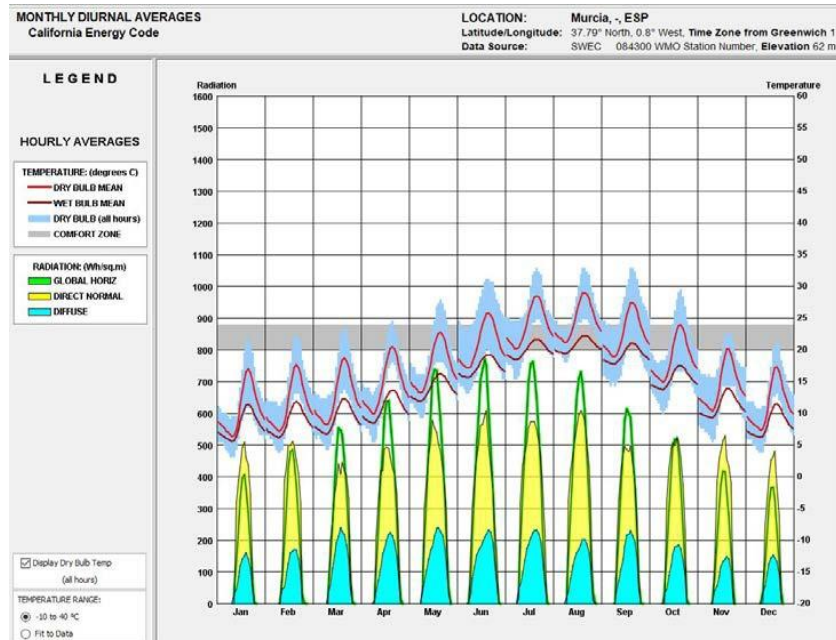


Figure 13. Simulation results: monthly average temperatures and radiation. Source: own elaboration using Climate Consultant 6.0 software.

Figure 14 shows the variation in solar radiation by surface, considering normal, horizontal and diffuse radiation.

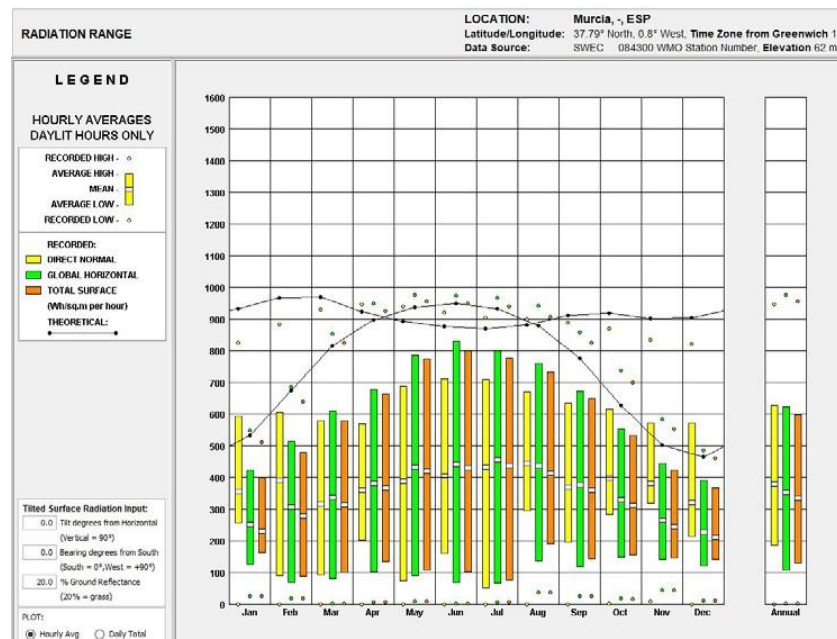


Figure 14. Simulation results: Radiation range. Source: own elaboration using Climate Consultant 6.0 software.

Figure 15a–c represent the mean sky coverage by cloud cover, the light intensity measured in lux, and the mean monthly wind speed measured in m/s, respectively.

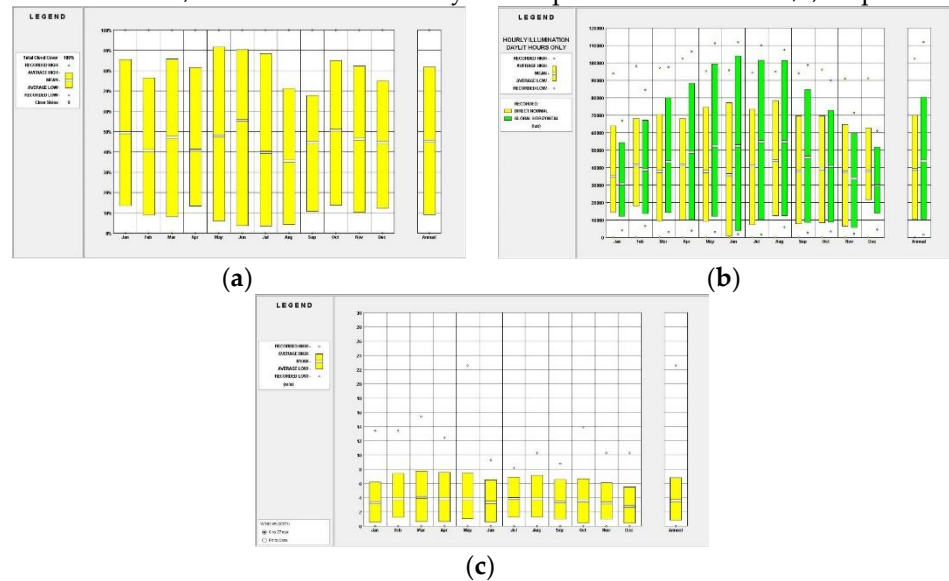


Figure 15. Simulation results: (a) mean sky coverage by cloudiness; (b) light intensity measured in lux; (c) mean monthly wind speed measured in m/s. Source: own elaboration using Climate Consultant 6.0 software.

Figure 16 represents the orientation and altitude of the sun for every 15 min of the year. The yellow zone indicates the comfort conditions as long as the dry bulb temperature is within the thermal comfort zone. The red zone indicates overheating when the dry bulb temperature is above the comfort zone. The blue zone represents cold conditions when the dry bulb temperature is below the comfort zone.

At the design level, in practice, it is important to note that openings (windows, openings, etc.) should be fully exposed to solar radiation if they are in the blue zone, while they should be fully shaded (no exposure to solar radiation) if they are in the red zone. The software itself integrates a tool that helps to make a pre-design for the win-

dows, allowing for the configuration of the most appropriate arrangement of the necessary solar protection in each case.

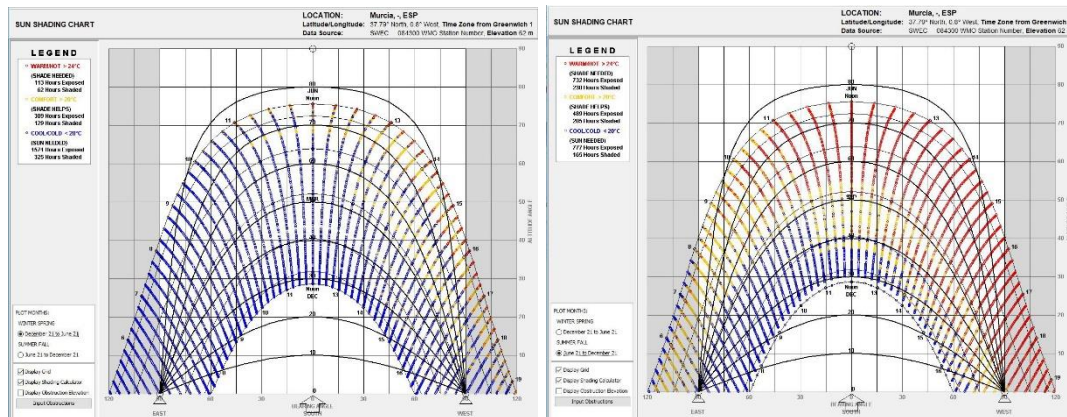


Figure 16. Simulation results: orientation and altitude of the sun for every 15 min of the year. Source: own elaboration using Climate Consultant software.

Figure 17 represents the psychrometric chart, as a confluence of three climatic attributes that influence the users' feelings of comfort. These three variables on the graph are the dry bulb temperature, wet bulb temperature and relative humidity. Their combination determines the different zones: above the comfort zone (red), below the comfort zone (blue) or within the comfort zone (green). On the other hand, this psychrometric chart can also be used to show how to design exterior enclosures that can modify or filter external climatic conditions to create more comfortable interior spaces.

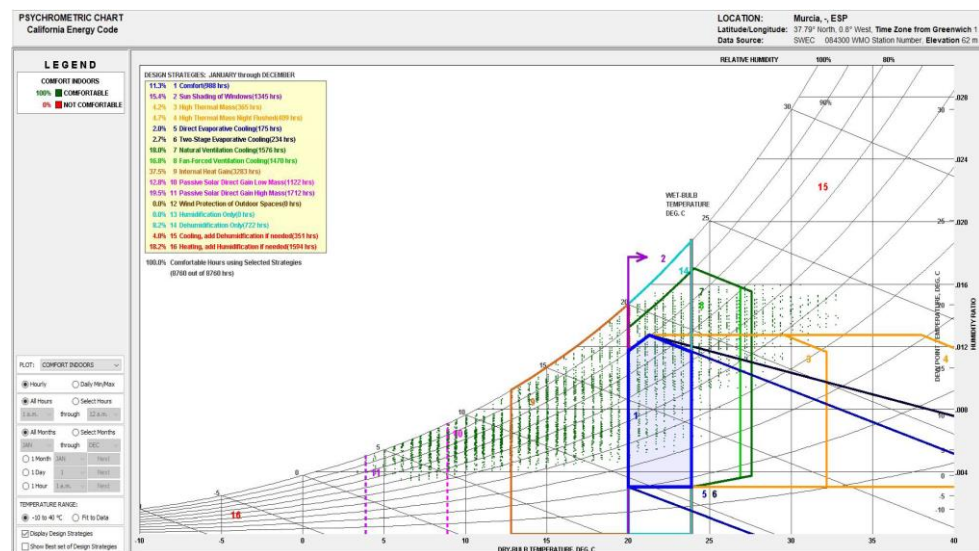


Figure 17. Simulation results: Murcia psychrometric chart. Source: own elaboration using Climate Consultant software.

Considering the site studied, the protection of the windows by shading, vegetation, eaves, etc., represents a 15.4% effectiveness in the design. This effectiveness refers to the number of hours of comfort gained within the living spaces designed in the interior. On the other hand, considering the climatic conditions, only 11.3% of the hours (988 h per year) are within the comfort range. The measures or design strategies indicated in the top left of the abacus in Figure 17 serve to improve these conditions by increasing the range of hours in comfort (Table 2).

Table 2. Design strategies from highest to lowest impact on indoor comfort.

DESIGN STRATEGIES				
37.50%	9	Internal heat gain	3283	hrs
19.50%	11	Passive solar direct gain high mass	1712	hrs
18.20%	16	Heating adds humidification (if needed)	1594	hrs
18%	7	Natural ventilation cooling	1576	hrs
16.80%	8	Fan-forced ventilation cooling	1470	hrs
15.40%	2	Sun shading of windows	1345	hrs
12.80%	10	Passive solar direct gain low mass	1122	hrs
11.30%	1	Comfort	988	hrs
8.20%	14	Dehumidification only	722	hrs
4.70%	4	High thermal mass night flushed	409	hrs
4.20%	3	High thermal mass	365	hrs
4.00%	15	Cooling adds dehumidification (if needed)	351	hrs
2.70%	6	Two-stage evaporative cooling	234	hrs
2.00%	5	Direct evaporative cooling	175	hrs
0.00%	12	Wind protection of outdoor spaces	0	hrs
0.00%	13	Humidification only	0	hrs

These strategies are evaluated from the highest to lowest impact on indoor comfort. Therefore, it is necessary to consider that, in relation to the gains from the domestic use of the space itself, the characteristic morphology of the geodesic domes will allow these gains to have an even greater impact, by facilitating and improving the movement of internal air in the space.

3.2. Study of Thermal Behaviour

3.2.1. Comparison of Parallelepiped and Geodesic Dome Geometry

The study of models 1 and 2 is carried out by applying the same environmental conditions and the same construction systems for a proper comparison of the resulting energy analysis with the Design Builder programme. Regardless of the material configuration of the envelope elements, it is essential to take into account the values of thermal transmittance (U), and to check that these values correspond to those reflected in the required thermal transmittance tables established in the CTE DB-HE 1 (Código Técnico de la Edificación, Documento Básico HE1 Limitación de la demanda energética) [76] for the climatic zone under study. The U value resulting from this envelope is $0.257 \text{ W/m}^2 \text{ K}$. The resulting U -value of the glazed part applying the ISO 15099/NFRC standard is $1.761 \text{ W/m}^2 \text{ K}$.

After the simulations are carried out, it can be seen that case study 2 (dome) invests 9% less in zone heating than case study 1 (reference block), due to the fact that the envelope behaves worse, generating more energy losses per square metre overall. The same is true for external ventilation, with case study 2 generating 9% less in losses than case study 1.

In relation to the cooling design, the energy and thermal envelope performance is analysed for an unfavourable summer day (July 15th) for both case study 1 (Figure 18) and case study 2 (Figure 19).

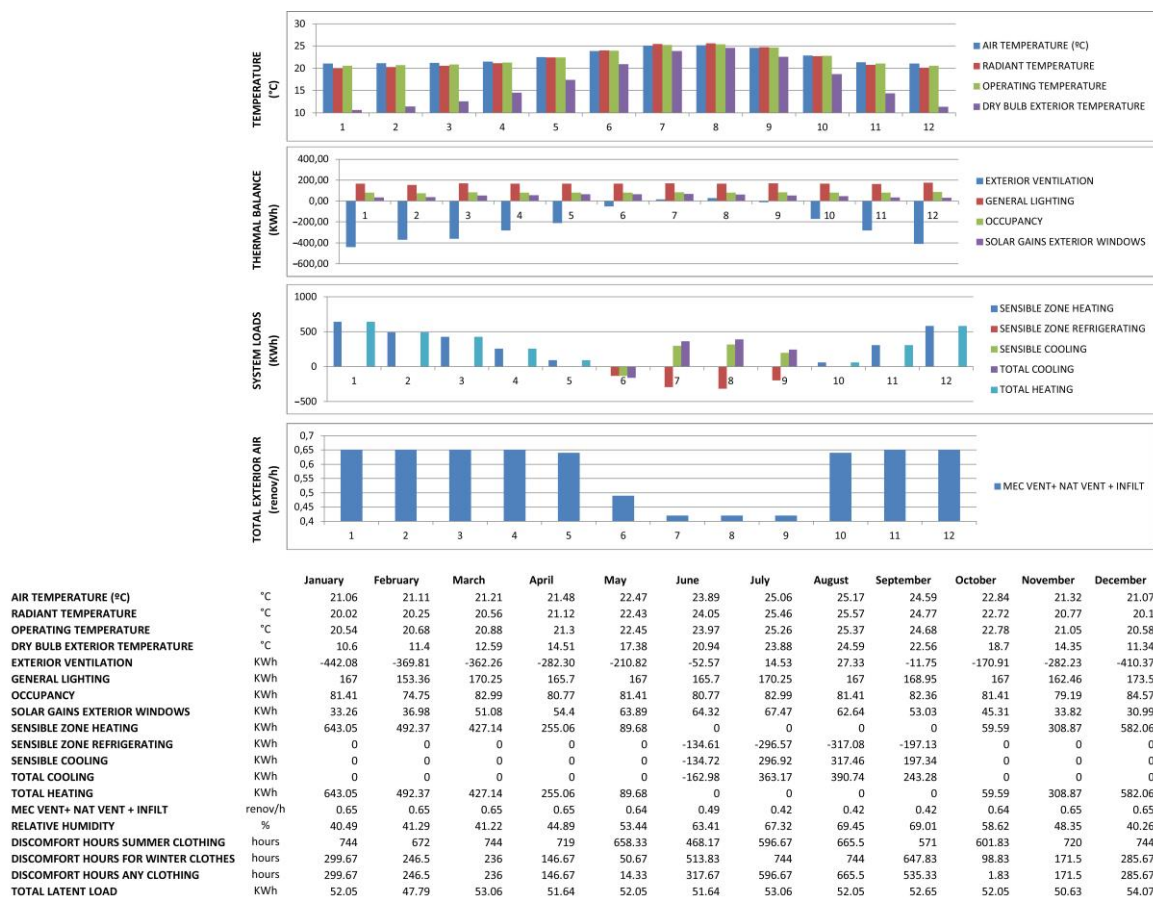
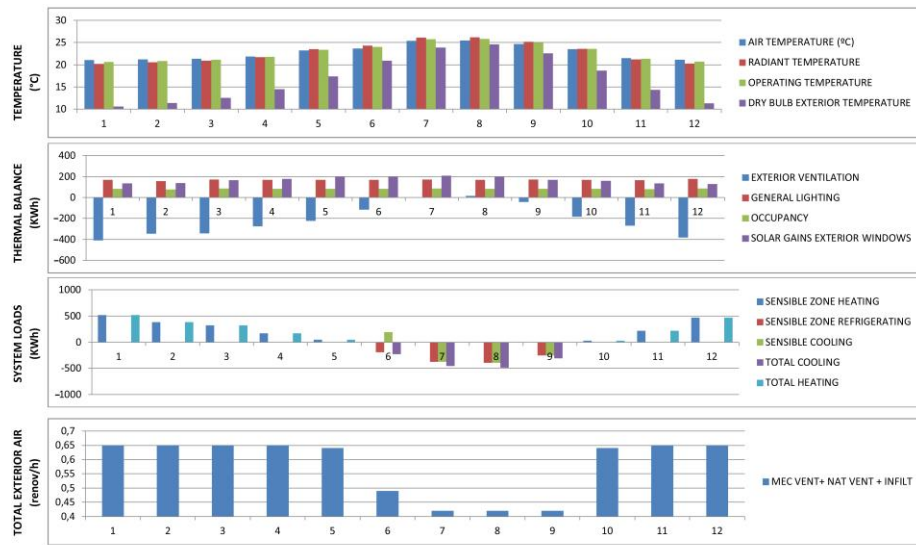


Figure 18. Simulation results for temperatures, internal and solar gains for case study 1.

The values obtained from both analyses have a dispersion of less than 3%, which indicates that the behaviour of both architectures is similar at coping with the cooling of the area. The major difference between the two cases lies in the distinction of building elements (wall cover). Case study 2, being a dome, has a structure composed of prefabricated modules throughout the envelope, which allows for an advantage against solar radiation due to the inclination of the faces.



	January	February	March	April	May	June	July	August	September	October	November	December
AIR TEMPERATURE (°C)	21.07	21.18	21.36	21.83	23.24	23.68	25.35	25.43	24.65	23.52	21.52	21.1
RADIANT TEMPERATURE	20.19	20.53	20.94	21.74	23.48	24.33	26.1	26.18	25.18	23.61	21.18	20.27
OPERATING TEMPERATURE	20.63	20.85	21.15	21.78	23.36	24	25.73	25.81	24.92	23.56	21.35	20.68
DRY BULB EXTERIOR TEMPERATURE	10.6	11.4	12.59	14.51	17.38	20.94	23.88	24.59	22.56	18.7	14.35	11.34
EXTERIOR VENTILATION	-410.37	-345.35	-341.71	-274.35	-224.71	-117.58	4.04	16.12	-42.51	-184.18	-268.81	-381.58
GENERAL LIGHTING	169.26	155.43	172.55	167.94	169.26	167.94	172.55	169.26	171.24	169.26	164.65	175.85
OCCUPANCY	82.5	75.76	84.11	81.86	82.5	81.86	84.11	82.5	83.47	82.5	80.26	85.72
SOLAR GAINS EXTERIOR WINDOWS	135.27	137.07	164.53	176.25	197.41	198.95	207.68	197.75	167.38	159.32	135.16	129.25
SENSITIVE ZONE HEATING	519.29	384.54	321.11	169.32	44.34	0	0	0	0	30.75	221.18	466.93
SENSITIVE ZONE REFRIGERATING	0	0	0	0	0	-192.2	-376.53	-395.59	-254.52	0	0	0
SENSIBLE COOLING	0	0	0	0	0	192.42	-377.14	-396.25	-254.91	0	0	0
TOTAL COOLING	0	0	0	0	0	-231.04	-458.09	-484.59	-312.04	0	0	0
TOTAL HEATING	519.29	384.54	321.11	169.32	44.34	0	0	0	0	30.75	221.18	466.93
MEC VENT+ NAT VENT + INFILT	0.65	0.65	0.65	0.65	0.64	0.49	0.42	0.42	0.42	0.64	0.65	0.65
RELATIVE HUMIDITY	%	40.76	41.43	41.18	44.29	51.35	62.05	64.88	66.92	67.27	56.6	48.07
DISCOMFORT HOURS SUMMER CLOTHING	hours	744	670.67	727.5	672.17	491	443	553.5	602.67	534.33	473	698.83
DISCOMFORT HOURS FOR WINTER CLOTHES	hours	298.83	242	230.17	150.5	205.33	488.83	744	643.83	236.5	173	282.83
DISCOMFORT HOURS ANY CLOTHING	hours	298.83	242	227	127.17	10	240.67	553.5	602.67	475.67	20.67	161.83
TOTAL LATENT LOAD	KWh	52.75	48.44	53.78	52.34	52.75	52.34	53.78	52.75	53.36	52.75	51.31

Figure 19. Simulation results for temperatures, internal and solar gains for case study 2 (geodesic dome).

Table 3 presents a comparative analysis of the data associated with case study 1 (reference block) and case study 2 (dome) for the annual energy simulation. The data are represented on a monthly basis in order to identify possible seasonal differences between the two analyses (although it is also possible to choose to represent the graphs on an annual or daily basis).

Table 3. Comparison of results.

	January	February	March	April	May	June	July	August	September	October	November	December	TO-TAL	
GENERAL LIGHTING	Case study 1 KWh	167	153.36	170.25	165.7	167	165.7	170.25	167	168.95	167	162.46	173.5	1998.17
	Case study 2 KWh	169.26	155.43	172.55	167.94	169.26	167.94	172.55	169.26	171.24	169.26	164.65	175.85	2025.19
OCCUPANCY	Case study 1 KWh	81.41	74.75	82.99	80.77	81.41	80.77	82.99	81.41	82.36	81.41	79.19	84.57	974.03
	Case study 2 KWh	82.5	75.76	84.11	81.86	82.5	81.86	84.11	82.5	83.47	82.5	80.26	85.72	987.15
SOLAR GAINS EXTERIOR WINDOWS	Case study 1 KWh	33.26	36.98	51.08	54.4	63.89	64.32	67.47	62.64	53.03	45.31	33.82	30.99	597.19
	Case study 2 KWh	135.27	137.07	164.53	176.25	197.41	198.95	207.68	197.75	167.38	159.32	135.16	129.25	2006.02
SENSIBLE ZONE HEATING	Case study 1 KWh	643.12	492.38	427.08	255.07	89.71	0	0	0	0	59.64	308.74	581.96	2857.70
	Case study 2 KWh	519.29	384.54	321.11	169.32	44.34	0	0	0	0	30.75	221.18	466.93	2157.46
SENSIBLE ZONE REFRIGERATING	Case study 1 KWh	0	0	0	0	0	-134.5	-296.3	-316.2	-197.05	0	0	0	-944.18
	Case study 2 KWh	0	0	0	0	0	-192.2	-376.5	-395.5	-254.52	0	0	0	-1218.8
RELATIVE HUMIDITY	Case study 1 %	40.49	41.29	41.22	44.89	53.44	63.41	67.32	69.45	69.01	58.62	48.35	40.26	53.15
	Case study 2 %	40.76	41.43	41.18	44.29	51.35	62.05	64.88	66.92	67.27	56.6	48.07	40.51	52.11
DISCOMFORT HOURS SUMMER CLOTHING	Case study 1 hours	744	672	744	719	658.33	468.17	596.67	665.5	571	601.83	720	744	7904.50

	Case study 2	hours	744	670.67	727.5	672.17	491	443	553.5	602.67	534.33	473	698.83	744	7354.67
DISCOMFORT HOURS FOR WINTER CLOTHES	Case study 1	hours	299.67	246.5	236	146.67	50.67	513.83	744	744	647.83	98.83	171.5	285.67	4185.17
	Case study 2	hours	298.83	242	230.17	150.5	205.33	488.83	744	744	643.83	236.5	173	282.83	4439.82
DISCOMFORT HOURS ANY CLOTHING	Case study 1	hours	299.67	246.5	236	146.67	14.33	317.67	596.67	665.5	535.33	1.83	171.5	285.67	3517.34
	Case study 2	hours	298.83	242	227	127.17	10	240.67	553.5	602.67	475.67	20.67	161.83	282.83	3242.84
TOTAL LATENT LOAD	Case study 1	KWh	52.05	47.79	53.06	51.64	52.05	51.64	53.06	52.05	52.65	52.05	50.63	54.07	622.74
	Case study 2	KWh	52.75	48.44	53.78	52.34	52.75	52.34	53.78	52.75	53.36	52.75	51.31	54.8	631.15

The air temperature, radiant temperature and operating temperature are slightly higher in case study 2 (dome) and are also more stable, with no significant differences in the average annual temperatures.

It is important to note that, due to its layout and geometry, the dome has a higher solar gain index (2006.02 kWh) compared to the reference block (597.19 kWh). Figure 20 shows the monthly differences between both case studies. Both constructions have the same façade treatment and orientation; however, the inclination of the dome modules directly affects this analysis. For this reason, the dome has a higher efficiency in colder months, but its geometry reduces its efficiency in warmer months as it receives a larger area of solar radiation. This variable makes a significant difference between the two geometries. Depending on the climate where it is located, solar control of the geodesic dome openings will be of vital importance for the best efficiency.

The general illumination, occupancy and latent load indices are maintained with very little dispersion between the two case studies. The relative humidity increases slightly in case 1 (reference block). The data show that the average annual relative humidity is 53.15% in case 1, while in case 2 it is 52.11% (dome).

In relation to the number of total hours of discomfort according to the type of clothing and month, it should be noted that, according to the conditions established for both cases, the result is 3517.34 total hours of discomfort for the reference block and 3242.84 total hours for case study 2 (dome). It should be noted that the hours of discomfort are more pronounced in the summer months, being lower in case study 2.

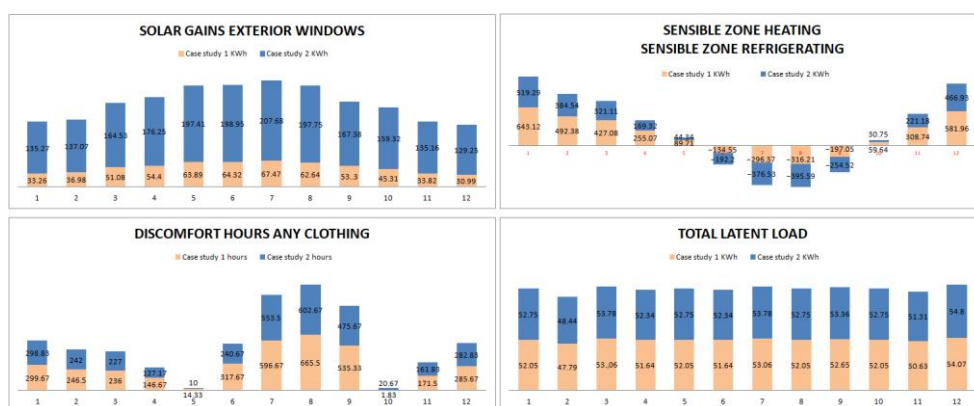


Figure 20. Simulation results for solar gains, heating and refrigerating, discomfort and latent load.

Electricity consumption between January and May and October and December is higher for the reference block than for the dome, due to heating needs. On the other hand, from June to September the cooling needs require a higher electricity consumption in the dome.

Regarding the overall consumption balance, it is possible to state that case 1 (traditional block) consumes more electricity throughout the year to maintain comfort conditions inside the house. In relation to fuel consumption, the CO₂ production graphs follow

the same balance for the different seasons, i.e., the higher the fuel demand, the higher the CO₂ impact.

Thus, so far, the results of the simulations have been analysed for the two main case studies: case 1 (simplified traditional architecture block) and case study 2 (geodesic dome). Neither of them has any defined type of uses or internal partitions, in order to check the behaviour related to the global building envelope under the same conditions as the internal heat gain.

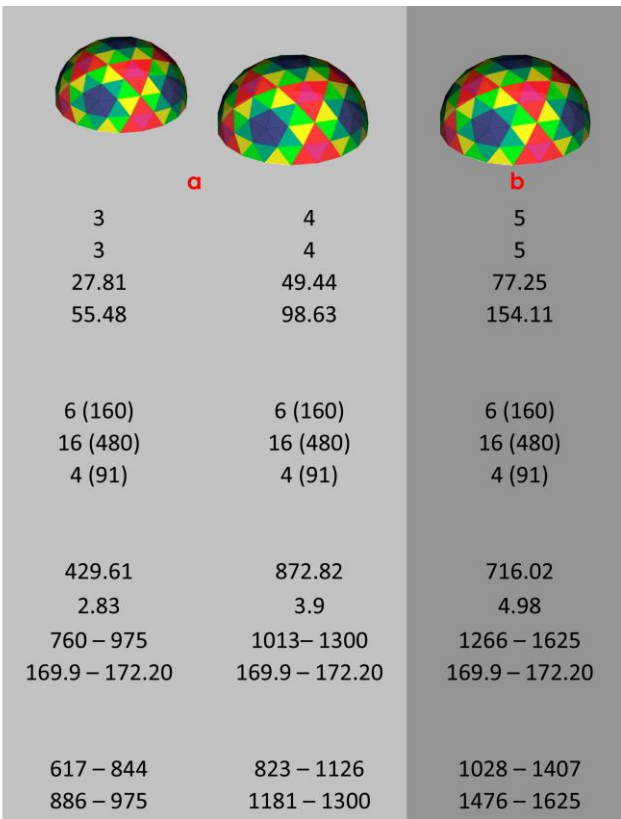
3.2.2. Comparison of the Single Geodesic Dome and Double Geodesic Dome

In this section, we will initially compare the geometries of both cases 2 and 3 to better understand their influence on energy efficiency.

Case study 2: The geodesic dome with a radius of 5 m contains an area of 77.25 m² (Figure 21b). When we divide this surface area into two domes with a radius of 3 m and 4 m (27.81 m² and 49.44 m², respectively), the surface area of 77.25 m² remains the same. It is important to remember that this surface area is the same as the reference block also studied (case study 1).

In a similar way, the envelope area remains unchanged. The 154.11 m² of roof in case 2 coincides with the sum of 55.48 m² and 98.63 m² of both domes in case 3 (Figure 21a).

In this way, the ratio of the occupied surface and envelope is maintained with respect to case 2 (single-dome model). However, it must be taken into account that the chimney effect in case 2 (single dome) causes more infiltration losses than in case 3 (two domes), as it has a lower height[77].



Height from base	m	3	4	5
Platform radius	m	3	4	5
Platform area,	m ²	27.81	49.44	77.25
Coverage area	m ²	55.48	98.63	154.11
Sizes (units)				
Faces		6 (160)	6 (160)	6 (160)
Edges		16 (480)	16 (480)	16 (480)
Vertices		4 (91)	4 (91)	4 (91)
Beams 150×50mm				
Total length of beams	m	429.61	872.82	716.02
Total volume of beams	m ³	2.83	3.9	4.98
Beam length	mm	760 – 975	1013 – 1300	1266 – 1625
Angle between faces	°	169.9 – 172.20	169.9 – 172.20	169.9 – 172.20
Triangles				
Min. Height	mm	617 – 844	823 – 1126	1028 – 1407
Max. Side	mm	886 – 975	1181 – 1300	1476 – 1625

Figure 21. Results for the surface area, coverage area, and beams of the two geodesic domes (3 m and 4 m. diameter, respectively) in case study 3 (a) and the single geodesic dome (5 m. diameter) in case study 2 (b).

There is one aspect of the geometry that does substantially modify the behaviour of one solution or the other: the length of the joints. The dome maintains its number of edges (480), but varies in the length of its edges and, thus, the length of its joints. The 5 m

radius dome has 29% less joint length than the sum of the 3 m and 4 m domes in case 3. In linear metres, we are talking about 716 m in case 2 versus 1.001 m (429 + 572) in case 3.

The division of case 2 versus case 3 allows for the distinction of uses. The simulation considers the existence of a differentiation of uses (night use and day use) and aims to check whether the division of uses into blocks of smaller volumetric dimensions affects the energy performance and, if so, analyses the implications. In addition, the internal heat gain changes when there are two spaces with different uses. In this sense, the research by Rainer Elstrand et al. [78] predicted that an increased ownership of appliances is the key driver of increased internal heat gains.

In case study 3, the reduction in the occupied volume is indeed significant, with a total occupied volume of 176.6 m³. In case study 2 (a single geodesic dome), this volume is 225 m³, and in the reference block it is 270 m³. With the same occupiable surface as the reference block, cases 2 and 3 reduce the interior volume by 83% and 65%.

After the geometric analysis, a detailed study of the energy performance of the two geodesic domes in case study 3 was carried out, and compared the results with those obtained for case study 2:

- Case 3 requires 24% less energy for lighting than case 2: 20,775 Wh/m² versus 27,060 Wh/m².
- Case 3 requires 52% less energy consumption for cooling than case 2: 5215 Wh/m² vs. 10,025 Wh/m².
- Case 3 requires 36% less energy loss for external ventilation than case 2: 22,086 Wh/m² compared to 34,293 Wh/m².
- The energy input for heating remains stable between case study 3 and case study 2.
- The discomfort hours remain stable between case study 3 and case study 2 for the set conditions.

As it is possible to set different zones of use in case study 3, the calculation parameters vary according to the imposed needs. In this case, considering the bedroom use and living room use separately for each block, the expenditure on lighting was recalculated, as was the expenditure for other sources of electricity consumption, obtaining an annual calculation of 60,966 Wh/m² for case study 3 that compared to 70,534 Wh/m² for case study 2, which represents an improvement of 14% in efficiency.

4. Discussion

The results presented in the previous section allow for a specific discussion of each study area, so that the geometric aspects, temperatures, solar gains and comfort hours can be analysed.

4.1. Comparative Analysis of the Geometry, Volume and Thermal Envelope

At the level of geometrical resolution, an interesting difference can be seen between case study 1 (reference block) and case study 2 (dome). Although the occupation surface is the same, 21% less envelope is required to cover the same needs. This characteristic has a direct impact on the material cost of the building per unit area. The load-bearing capacity of both structures or the need for auxiliary means is also significant, although this is not the aim of this research.

The volume delimited by reference block 1 is the largest one (270 m³ for a clear height of 3.5 m). The use of a geodesic dome of frequency IV 1/2 with a radius of 5m and 5m height implies a saving of 17% in volume. Frequencies III 5/12 and III 7/12 significantly reduce this aspect compared to the frequency type IV 1/2 studied.

The comparison of the volumes between case 2 and case 3 is significant. Case study 3 has a total volume of 176.6 m³, while maintaining the same total area for occupation. In case study 2, which consists of a single geodesic dome, the volume is 225 m³. Case 3, with a dome of 3 m in height and another of 4m in height, 4m represents a 22% savings in volume compared to case 2, with a dome of 5 m in height. In other words, the use of ge-

odesic domes with differentiated uses allows for a savings of 35% in volume for the same occupied surface area. It is true that the division into two uses, day and night, restricts the design possibilities, by reducing the free 5 m height of a single dome into separated 4 m and 3 m domes. However, at the same time, it has a very positive impact on consumption, as it means less consumption for heating and cooling.

4.2. Indoor Temperatures

Figure 17 shows that the range of dry bulb temperatures that provide comfort is between 20 °C and 24 °C, with humidity levels between 20 and 80%. Therefore, the setpoint values in DesignBuilder are set accordingly. The preset values (20 °C indoor temperature for heating with a setpoint temperature of 19 °C, and 24 °C indoor temperature for cooling with a setpoint temperature of 27 °C) strongly influence the hours of comfort and discomfort.

The maximum temperature for the extended comfort zone during summer is 29 °C, with humidity levels ranging from 20% to 80%. With mass cooling, the temperature can reach up to 31 °C, provided that the humidity remains between 5% and 80%. However, it should be noted that neither of these premises have been conclusively established.

4.3. Solar Gains

The geometry of the geodesic domes analysed maximises their capacity to capture solar radiation throughout the day. The solar gains for the month of January for reference block 1 (33.26 KWh) are almost five times lower than those for case study 2 (135.27 KWh). These solar gains are especially interesting in climates such as the BSh, due to its high annual insolation [79]. Therefore, in this type of climate, the geometric characteristics of the geodesic domes make it possible to greatly reduce the energy demand in winter. July is the month with the greatest gain in case study 1 (67.47 KWh), almost doubling the value for January. The gain for the same month in case study 2 (207.68 kWh) is more than three times higher. The annual calculation maintains a similar proportion: it is 597.19 KWh for case 1 compared to 2006.02 KWh for case study 2. This gives the geodesic dome a higher solar gain that can be used during the cold months, but also makes it necessary to protect the dome during the warm months in order to control its efficiency.

Case studies 2 and 3 generate a better distribution of sunlight and a higher uniformity compared to the reference block. This also has an impact on the lighting, as it is possible to make a better use of the natural lighting needs inside the building throughout the day over the entire surface area.

Following the data provided in the simulations, it has been found that, without entailing an increase in material cost execution, dividing the occupied surface area into uses (case study 3) allows for greater control of the resources derived from solar radiation and external ventilation compared to case 1 and case 2. This makes it possible to reduce energy consumption and obtain a more energy-efficient project.

4.4. Energy Efficiency

For warmer months, the efficiency of case 3 (60,966.47 Wh/m²) compared to case 2 (70,534.69 Wh/m²) is considerable in terms of cooling, as it is possible to control the solar incidence and solar radiation by separate blocks, thus optimising the available resources. It has been possible to demonstrate the estimation proposed by Soares [42] for the construction of hotel rooms with geodesic domes. The electricity consumption in case 3 is reduced in the annual calculation. The use of a double dome consumes less energy, as it has to cool a smaller volume, provided that the air infiltration and insulation are controlled. Considering this, it is not only necessary to consider the U-value of the cladding materials, but also the way in which they age. Figure 22 shows the deformation of the cellulose. It reduces in volume over time due to the effect of moisture, if there is an excessive water vapour permeability of the cladding layers.



Figure 22. Image of the deformation of the cellulose inside the enclosure.

The balance between the geometry, volume and use of the space in a dome can improve the efficiency of this type of architecture. Acting on the overall length of the joints, the optimal orientation of the windows and the adequate solar protection of its glazing in summer would allow for a reduction in heating and cooling consumption, as well as in the overall electricity consumption of case study 3 compared to case study 2.

5. Conclusions

From the studies carried out in the present research in relation to energy efficiency applied to geodesic dome envelopes, it is possible to conclude that:

- The most influential strategies for improving energy efficiency, such as direct passive solar gain, heating, natural ventilation cooling, fan-forced ventilation cooling and the solar shading of windows, allow for geodesic domes to be one of the most efficient geometries.
- In small spaces such as tourist accommodations, the examples studied allow for a greater optimisation of resources than conventional solutions. The research confirms that incorporating domes into the architectural design of tourist accommodations improves its energy performance.
- The reduction in occupied volume is indeed significant. With the same occupiable surface as the reference block, a single and a double geodesic dome reduce the interior volume by 83% and 65%, respectively. A more detailed study of the relationship between the surface area and different uses would allow for a more precise quantification of their impact on this type of architecture.
- It is confirmed that the use of differentiated day and night spaces in geodesic domes improves the energy performance by requiring 24% less energy for lighting and 52% less energy consumption for cooling, compared to other conventional examples with the same surface area.
- The most unfavourable case of domes was for the highest number of joints (712), those of frequency IV. A more detailed study of the infiltrations for dome frequencies IV, III 5/12 and III 7/12 would further improve the energy efficiency of the dome with respect to the parallelepiped geometry considered in this research. The choice of a small frequency for the design of a geodesic dome allows for less infiltrations. An intensive execution control would ensure that these infiltrations would not affect the results obtained in the software calculation.
- In order to correctly model the geometry of a geodesic dome, different software has been necessary. Autodesk REVIT needs further development to generate more complex analytical volumes. This makes it difficult to read the calculation program's results, and the associated parametric information is lost in the process. The high difficulty regarding the interoperability between different modelling and energy calculation software makes the analysis process for this type of singular geometry more difficult, due to incompatibilities in the export of files between the software.

Author Contributions: Conceptualization, C.P.-C. and M.I.P.-M.; methodology, C.P.-C. and Á.B.G.-A.; software, C.P.-C. and A.G.-G.; validation, C.P.-C. and A.G.-G.; formal analysis, M.I.P.-M.; investigation, C.P.-C., Á.B.G.-A. and A.G.-G.; resources, M.I.P.-M.; data curation, C.P.-C. and M.I.P.-M.; writing—original draft preparation, C.P.-C. and M.I.P.-M.; writing—review and editing, Á.B.G.-A. and A.G.-G.; visualization, C.P.-C. and M.I.P.-M.; supervision, C.P.-C. and A.G.-G.; project administration, C.P.-C. All authors have read and agreed to the published version of the manuscript.

Funding: This research received no external funding

Data Availability Statement: The data presented in this study are available on request from the corresponding author.

Acknowledgments: We acknowledge the origin of this research was the final degree work of Mark Sanshi Hamaoka, directed by Angel Benigno González and Antonio Galiano.

Conflicts of Interest: The authors declare no conflicts of interest.

References

1. Beaver, A. *A Dictionary of Travel and Tourism*; Oxford University Press: Oxford, UK, 2012.
2. Horáková, H.; Boscoboinik, A. (Eds.) *From Production to Consumption: Transformation of Rural Communities*; LIT Verlag: Münster, Germany, 2012.
3. Gössling, S.; Scott, D.; Hall, C.M. Pandemics, Tourism and Global Change: A Rapid Assessment of COVID-19. *J. Sustain. Tour.* **2021**, *29*, 1–20. <https://doi.org/10.1080/09669582.2020.1758708>.
4. Craig, C.A.; Karabas, I. Glamping after the Coronavirus Pandemic. *Tour. Hosp. Res.* **2021**, *21*, 251–256. <https://doi.org/10.1177/1467358421993864>.
5. Milohnić, I.; Cvelić Bonifačić, J.; Licul, I. Transformation of Camping into Glamping—Trends and Perspectives. *ToSEE Tour. South. East. Eur.* **2019**, *5*, 457–473. <https://doi.org/10.20867/tosee.05.30>.
6. Europe Glamping Market Size, Share & Growth. 2023. Available online: <https://www.grandviewresearch.com/industry-analysis/europe-glamping-market-report> (accessed on 26 May 2023).
7. Claver-Cortés, E.; Molina-Azorín, J.F.; Pereira-Moliner, J.; López-Gamero, M.D. Environmental Strategies and Their Impact on Hotel Performance. *J. Sustain. Tour.* **2007**, *15*, 663–679. <https://doi.org/10.2167/jost640.0>.
8. Blanco, E.; Rey-Maqueira, J.; Lozano, J. Economic Incentives for Tourism Firms to Undertake Voluntary Environmental Management. *Tour. Manag.* **2009**, *30*, 112–122. <https://doi.org/10.1016/j.tourman.2008.04.007>.
9. Alonso-Almeida, M.-M.; Fernández Robin, C.; Celemin Pedroche, M.S.; Astorga, P.S. Revisiting Green Practices in the Hotel Industry: A Comparison between Mature and Emerging Destinations. *J. Clean. Prod.* **2017**, *140*, 1415–1428. <https://doi.org/10.1016/j.jclepro.2016.10.010>.
10. Kostakis, I.; Sardianou, E. Which Factors Affect the Willingness of Tourists to Pay for Renewable Energy? *Renew. Energy* **2012**, *38*, 169–172. <https://doi.org/10.1016/j.renene.2011.07.022>.
11. Çelik, N.; Bahar, O.; Tatar, S. The role of glamping tourism in rural development: The case of Club Amazon Bordubet. *J. Int. Soc. Res.* **2017**, *10*, 1282–1287. <https://doi.org/10.17719/jisr.2017.1855>.
12. Boscoboinik, A.; Bourquard, E. Glamping and Rural Imaginary. In *From Production to Consumption: Transformation of Rural Communities*; LIT Verlag: Münster, Germany, 2012; pp. 149–164.
13. Lucivero, M. Camping and Open-Air Tourism: An Opportunity for Sustainable Tourism in Coastal Areas. In *Proceedings of the 6th Conference of the International Forum on Urbanism (IFoU): TOURBANISM, Barcelona, Spain, 25–27 January 2012*; International Forum on Urbanism: Barcelona, Spain, 2012; pp 1–9.
14. Brooker, E.; Joppe, M. Trends in Camping and Outdoor Hospitality—An International Review. *J. Outdoor Recreat. Tour.* **2013**, *3–4*, 1–6. <https://doi.org/10.1016/j.jort.2013.04.005>.
15. ArchDaily en Español. Hotel Tenir Eco/Levelstudio. Available online: <https://www.archdaily.cl/cl/957587/hotel-tenir-eco-levelstudio> (accessed on 11 January 2024).
16. ArchDaily. DOM(E)/NRJA. Available online: https://www.archdaily.com/382876/dom-e-nrja?ad_source=search&ad_medium=projects_tab (accessed on 11 January 2024).
17. ArchDaily en Español. Vivienda Modular Labt 20 (10,5) City Bell/Estudio Borrachia + GB Arquitectos. Available online: https://www.archdaily.cl/cl/1000180/vivienda-modular-labt-20-estudio-borrachia-arquitectos-plus-gb-arquitectos?ad_source=search&ad_medium=projects_tab (accessed on 11 January 2024).
18. ArchDaily en Español. Vivienda Geodésica/Ecoprojecta. Available online: https://www.archdaily.cl/cl/805836/vivienda-geodesica-ecoprojecta?ad_source=search&ad_medium=projects_tab (accessed on 11 January 2024).
19. Arquitectura. CASA M + J de Manuel Cerdá. Un Refugio Suficiente. Available online: <https://arquitecturayempresa.es/noticia/casa-mj-de-manuel-cerda-un-refugio-suficiente> (accessed on 11 January 2024).

20. ArchDaily en Español. Sauna Sazae/Kengo Kuma & Associates. Available online: https://www.archdaily.cl/cl/995394/sauna-sazae-kengo-kuma-and-associates?ad_source=search&ad_medium=projects_tab (accessed on 11 January 2024).
21. ArchDaily. Ranwu Lake Campsite/Archermit. Available online: <https://www.archdaily.com/877966/ranwu-lake-campsite-xiao-yin-architecture-design-firm> (accessed on 11 January 2024).
22. ArchDaily en Español. Dos Domos y un Zócalo: Casa 8 por B + V Arquitectos. Available online: https://www.archdaily.cl/cl/761630/dos-domos-y-un-zocalo-casa-8-por-b-plus-v-arquitectos?ad_source=search&ad_medium=projects_tab (accessed on 11 January 2024).
23. ArchDaily en Español. Casa Cambará Container/Estúdio Saymon Dall Alba + Mégui Dal Bó Arquiteta. Available online: <https://www.archdaily.cl/cl/932793/casa-cambara-container-saymon-dall-alba-arquiteto-plus-megui-dal-bo-arquiteta> (accessed on 11 January 2024).
24. ArchDaily en Español. Katerina Gordon. En Construcción: Domo Cluster/Arketiposchile. 2012. Available online: <https://www.archdaily.cl/cl/02-165500/en-construccion-domo-cluster-arketiposchile> (accessed on 20 November 2023).
25. Bysiec, D.; Jaszczynski, S.; Maleska, T. Analysis of Lightweight Structure Mesh Topology of Geodesic Domes. *Appl. Sci.* **2024**, *14*, 132. <https://doi.org/10.3390/app14010132>.
26. Kubik, M.; Augarde, C. *Structural Analysis of Geodesic Domes*; Durham University: Durham, UK, 2009.
27. Tarnai, T. Geodesic Domes: Natural and Man-Made. *Int. J. Space Struct.* **2011**, *26*, 215–227. <https://doi.org/10.1260/0266-3511.26.3.215>.
28. Kolpakov, A.; Dolgov, O.; Korolskiy, V.; Popov, S.; Anchutin, V.; Zykov, V. Analysis of Structural Layouts of Geodesic Dome Structures with Bar Filler Considering Air Transportation. *Buildings* **2022**, *12*, 242. <https://doi.org/10.3390/buildings12020242>.
29. Heidari, A.; Olivieri, F. Energy Efficiency in Dome Structures: An Examination of Thermal Performance in Iranian Architecture. *Buildings* **2023**, *13*, 2171. <https://doi.org/10.3390/buildings13092171>.
30. Kermatigo, W.; Masruchin, F. Implementation of Domes Building in Simoketawang Village Tourism Education Facilities, Sidoarjo City. *Asian J. Soc. Humanit.* **2023**, *1*, 375–383. <https://doi.org/10.59888/ajosh.v1i108.52>.
31. *DesignBuilder*, version v.7.0.1.006; DesignBuilder Software Ltd.: Stroud, UK, 2023. Available online: <https://designbuilder.co.uk/> (accessed on 29 November 2023).
32. *EnergyPlus*, v.23.1.0; U.S. Department of Energy's (DOE) Building Technologies Office (BTO): Washington, DC, USA, 2023. Available online: <https://energyplus.net/> (accessed on 29 November 2023).
33. HiSoUR Arte Cultura Historia. Cúpula Geodésica. Available online: <https://www.hisour.com/es/geodesic-dome-32059/> (accessed on 29 November 2023).
34. Sutton, D. *Sólidos Platónicos y Arquimedianos*; Ediciones Oniro: Barcelona, Spain, 2005.
35. Gaspar, O. Bauersfeld's Concept for the Subdivision of the First Built Geodesic Dome Structure. In Proceedings of the IASS Annual Symposium 2020/21 and the 7th International Conference on Spatial Structures—Inspiring the Next Generation, Guildford, UK, 23–27 August 2021.
36. Chu, H.-Y. The Evolution of the Fuller Geodesic Dome: From Black Mountain to Drop City. *Des. Cult.* **2018**, *10*, 121–137. <https://doi.org/10.1080/17547075.2018.1466228>.
37. Díaz, E. *The Experimenters: Chance and Design at Black Mountain College*; The University of Chicago Press: Chicago, IL, USA; London, UK, 2015.
38. Buckminster Fuller, R. Building Construction. U.S. Patent US2682235A, 26 June 1954. Available online: <https://patents.google.com/patent/US2682235?q=2682235> (accessed on 13 May 2023).
39. de Lózar de la Viña, M. Casa Cúpula En Carbondale, Illinois. R. B. Fuller, 1960. *ARQ* **2013**, *84*, 14–27. <https://doi.org/10.4067/S0717-69962013000200003>.
40. Peñalver Oltra, M. Estudio de Alternativas de Cúpula Geodésica En Madera de Fácil Realización y Montaje. Bachelor's Thesis, Valencia Polytechnic University, Valencia, Spain, 2017.
41. South, H.; Harris, M.E. Black Mountain College Project Collection. Western Regional Archives, 3rd floor stacks, Row 5. p 25 boxes. Available online: <https://archives.ncdcr.gov/documents/black-mountain-college-project-inventory/open> (accessed on 29 November 2023).
42. Soares, T.; Arruda, A. As estruturas geodésicas do Ecocamp na Patagônia: Um estudo sobre seus aspectos ergonômicos e sustentáveis. *Blucher Eng. Proc.* **2016**, *3*, 216–227. <https://doi.org/10.5151/engpro-conaerg2016-9039>.
43. Weisstein, E.W. Polyhedral Formula. Available online: <https://mathworld.wolfram.com/PolyhedralFormula.html> (accessed on).
44. Kitrick, C.J. A Unified Approach to Class I, II & III Geodesic Domes. *Int. J. Space Struct.* **1990**, *5*, 223–246. <https://doi.org/10.1177/026635119000500307>.
45. Barba Marcos, J. Cúpula Geodésica Destinada a la Implantación de Huertos Urbanos. Bachelor's Thesis, University Charles III of Madrid, Madrid, Spain, 2015.
46. CORE. Estudio Paramétrico de Cúpulas de Barras: Generación Paramétrica, Cálculo Automatizado y Comparativa del Comportamiento de Cúpulas de Haces ante Variaciones Geométricas. Available online: <https://core.ac.uk/display/61917800?source=2> (accessed on 13 May 2023).
47. Stasi, G. Geometrías Geodésicas y Sistemas Constructivos: Diseño e Implementación de Sistemas Low-Tech. Ph.D. Thesis, University of Seville, Seville, Spain, 2018.
48. Shelter Doms. Doms pare Glamping. Available online: <https://shelter-dome.com/case/> (accessed on 13 May 2023).

49. Martín-Pastor, A.; Martín-Mariscal, A.; López-Martínez, A. Self-Built Geodesic Geometries. In Proceedings of the 3rd International Congress on Sustainable Construction and Eco-Efficient Solutions, Seville, Spain, 27–29 March 2017; pp. 168–191. <https://doi.org/10.5281/zenodo.1297169>.
50. Ecoproyecto. Cúpulas Geodésicas. Available online: <https://ecoproyecto.es/cupulas-geodesicas/> (accessed on).
51. Porta-Gándara, M. A.; Gómez-Muñoz, V. Solar Performance of an Electrochromic Geodesic Dome Roof. *Energy* **2005**, *30*, 2474–2486. <https://doi.org/10.1016/j.energy.2004.12.001>.
52. 06/00879 Solar Performance of an Electrochromic Geodesic Dome Roof: Porta-Gándara, M. A. and Gómez-Muñoz, V. *Energy*, **2005**, *30*, (13), 2474–2486. *Fuel Energy Abstr.* **2006**, *47*, 129. [https://doi.org/10.1016/S0140-6701\(06\)80881-7](https://doi.org/10.1016/S0140-6701(06)80881-7).
53. Haghazadeh, R.; Nooshin, H.; Golabchi, M. Improving the Regularity of Geodesic Domes Using the Concept of Stepping Projection. *Int. J. Space Struct.* **2014**, *29*, 81–95. <https://doi.org/10.1260/0266-3511.29.2.81>.
54. Saka, M.P. Optimum Geometry Design of Geodesic Domes Using Harmony Search Algorithm. *Adv. Struct. Eng.* **2007**, *10*, 595–606. <https://doi.org/10.1260/136943307783571445>.
55. Fuller, R.B.; Applewhite, E.J. *Synergetics: Explorations in the Geometry of Thinking*; Macmillan: New York, NY, USA, 1975. Available online: <https://philpapers.org/rec/FULSEI> (accessed 3 January 2024).
56. Laila, T.; Arruda, A.; Barbosa, J.; Moura, E. The Constructive Advantages of Buckminster Fuller’s Geodesic Domes and Their Relationship to the Built Environment Ergonomics. In *Advances in Ergonomics in Design—Proceedings of the AHFE 2017 International Conference on Ergonomics in Design, Los Angeles, CA, USA, 17–21 July 2017*; Advances in Intelligent Systems and Computing; Springer: Cham, Switzerland, 2018; Volume 588, pp. 359–368. https://doi.org/10.1007/978-3-319-60582-1_36.
57. Soares, T.; Arruda, A. Geodesic Domes as Business Model in Hotel Management for Local Economies Development. *Cent. Estud. Diseño Comun.* **2020**, *80*, 111–122.
58. Pastukh, O.; Zhiyotov, D.; Vaitens, A.; Yablonskii, L. The Use of Modern Polymer Materials and Wood in the Construction of Buildings in the Form of Geodesic Domes. *E3S Web Conf.* **2021**, *274*, 1024. <https://doi.org/10.1051/e3sconf/202127401024>.
59. ArchDaily en Español. Available online: https://www.archdaily.cl/cl?ad_name=small-logo (accessed on 2 October 2023).
60. Pérez Aranda, A.; Arco Díaz, J.; Hidalgo García, D. Energy Study of the Envelope in Metal Containers for Building = Estudio Energético de La Envolvente En Contenedores Metálicos Para Edificación. *Build. Manag.* **2019**, *3*, 36–48. <https://doi.org/10.20868/BMA.2019.1.3875>.
61. Freitas, G.; Rabelo, E.; Pessoa, E. Projeto Modular Com Reaproveitamento de Container Maritimo. *Braz. J. Dev.* **2023**, *9*, 24368–24404. <https://doi.org/10.34117/bjdv9n10-057>.
62. Bernardo, L.; Pereira de Oliveira, L.; Nepomuceno, M.; Andrade, J. Use of Refurbished Shipping Containers for the Construction of Housing Buildings: Details for the Structural Project. *J. Civ. Eng. Manag.* **2013**, *19*, 628–646. <https://doi.org/10.3846/13923730.2013.795185>.
63. Laksitoadi, B.; Hasan, M. Refurbished Shipping Containers as Architectural Module in Bandung. In *Proceedings of the 3rd International Conference on Dwelling Form (IDWELL 2020), Online, 27–28 October 2020*; Atlantis Press: Amsterdam, The Netherlands, 2020. <https://doi.org/10.2991/assehr.k.201009.001>.
64. Pilarska, D.; Maleska, T. Numerical Analysis of Steel Geodesic Dome under Seismic Excitations. *Materials* **2021**, *14*, 4493. <https://doi.org/10.3390/ma14164493>.
65. Carvalho, J.P.G.; Lemonge, A.C.C.; Hallak, P.H.; Vargas, D.E.C. Simultaneous Sizing, Shape, and Layout Optimization and Automatic Member Grouping of Dome Structures. *Structures* **2020**, *28*, 2188–2202. <https://doi.org/10.1016/j.istruc.2020.10.016>.
66. Szmít, R. Geometry Design and Structural Analysis of Steel Single-Layer Geodesic Domes. In Proceedings of the 2017 Baltic Geodetic Congress (BGC Geomatics), Gdansk, Poland, 22–25 June 2017; pp. 205–209. <https://doi.org/10.1109/bgc.geomatics.2017.9>.
67. Gholizadeh, S.; Barati, H. Topology Optimization of Nonlinear Single Layer Domes by a New Metaheuristic. *Steel Compos. Struct. Int. J.* **2014**, *16*, 681–701.
68. Kaveh, A.; Rezaei, M. Topology and Geometry Optimization of Single-Layer Domes Utilizing CBO and ECBO. *Sci. Iran.* **2016**, *23*, 535–547. <https://doi.org/10.24200/SCI.2016.2137>.
69. Monolithic.org. The Inn Place—New Rentals, Old Pattern. Available online: <https://www.monolithic.org/rentals/the-inn-place-new-rentals-old-pattern> (accessed on 1 November 2023).
70. 7/12 Kruschke GoodKarma 3V R2.2 Beams 120x40—Geodesic Dome Calculator—Acidome.ru. Available online: https://acidome.com/lab/calc/#7/12_Kruschke_GoodKarma_3V_R2.2_beams_120x40 (accessed on 2 October 2023).
71. Otero, C.; Díaz, J.; Togores Fernández, R.; Manchado, C. Chordal Space Structures, Shaped from Voronoi Diagrams. In Proceedings of the Joint International Conference on Computing and Decision Making in Civil and Building Engineering, Montreal, QC, Canada, 14–16 June 2006.
72. Vrontissi, M.; Azariadi, S. Digital Tools in the Architectural Design of a Geodesic Dome: The Case-Study of the Bearing Structure of an Artificial Sky Lighting Installation. In *Respecting Fragile Places—Proceedings of the 29th Conference on Education in Computer Aided Architectural Design in Europe (eCAADe 2011), Ljubljana, Slovenia, 21–24 September 2011*; Education in Computer Aided Architectural Design in Europe (eCAADe): Brussels, Belgium; Faculty of Architecture: Ljubljana, Slovenia, 2011. <https://doi.org/10.52842/conf.ecaade.2011.511>.
73. DesignBuilder. Aurea Consulting. Available online: <https://ecoficiente.es/designbuilder/> (accessed on 13 May 2023).

74. ASHRAE. Thermal Environmental Conditions for Human Occupancy; ASHRAE Standard 55-2023; ASHRAE: Atlanta, GA, USA, 2023. Available online: <https://www.ashrae.org/technical-resources/bookstore/standard-55-thermal-environmental-conditions-for-human-occupancy> (accessed on 23 October 2023).
75. Espín-Sánchez, D.; Olcina-Cantos, J.; Conesa-García, C. Temporal Changes in Tourists' Climate-Based Comfort in the South-eastern Coastal Region of Spain. *Climate* **2023**, *11*, 230. <https://doi.org/10.3390/cli11110230>.
76. Código Técnico de la Edificación. *Documento Básico de Ahorro de Energía*; Ministerio de Transportes, Movilidad y Agenda Urbana: Madrid, Spain, 2022.
77. Garcilópez Gracia, E. J.; Romeo Giménez, L.M. *Evaluación de Las Infiltraciones En La Edificación y Aplicación Al Edificio Del Solar Decathlon*; Universidad de Zaragoza: Zaragoza, Spain, 2010.
78. Elsland, R.; Peksen, I.; Wietschel, M. Are Internal Heat Gains Underestimated in Thermal Performance Evaluation of Buildings? *Energy Procedia* **2014**, *62*, 32–41. <https://doi.org/10.1016/J.EGYPRO.2014.12.364>.
79. Pérez-Carramiñana, C.; Sabatell-Canales, S.; González-Avilés, Á.B.; Galiano-Garrigós, A. Influence of Spanish Energy-Saving Standard on Thermal Comfort and Energy Efficiency Owing to the War in Ukraine: Case Study of an Office Building in a Dry Mediterranean Climate. *Buildings* **2023**, *13*, 2102. <https://doi.org/10.3390/buildings13082102>.

Disclaimer/Publisher's Note: The statements, opinions and data contained in all publications are solely those of the individual author(s) and contributor(s) and not of MDPI and/or the editor(s). MDPI and/or the editor(s) disclaim responsibility for any injury to people or property resulting from any ideas, methods, instructions or products referred to in the content.